Coupling with the Jahn–Teller mode for triplet states of MF(6) (M=Mn2+,Cr3+) complexes: Dependence on the M–F distance and influence on the Stokes shift

ARTICLE *in* PHYSICA STATUS SOLIDI (B) · JULY 1996

Impact Factor: 1.49 · DOI: 10.1002/pssb.2221960119

3 AUTHORS, INCLUDING:

Miguel Moreno
Universidad de Cantabria

224 PUBLICATIONS **2,707** CITATIONS

SEE PROFILE

phys. stat. sol. (b) **196**, 193 (1996)

Subject classification: 71.10 and 71.70; 78.55; S9

Departamento de Física Moderna (a) and
Departamento de Ciencias de la Tierra y Física de la Materia Condensada (b),
Facultad de Ciencías, Universidad de Cantabria, Santander[1])

Coupling with the Jahn-Teller Mode for Triplet States of MF_6 ($M = Mn^{2+}$, Cr^{3+}) Complexes: Dependence on the M–F Distance and Influence on the Stokes Shift

By

M. T. BARRIUSO (a), J. A. ARAMBURU (b), and M. MORENO (b)

(Received July 11, 1995; in revised form February 26, 1996)

The microscopic origin of the V_E coupling constant with the Jahn-Teller mode E_g for orbital triplet states corresponding to several excited states of MnF_6^{4-} and the $^4T_{2g}$ state of CrF_6^{3-} is explored by molecular orbital (MO) calculations. V_E is shown to be determined by the splittings Δ_e and Δ_t induced in the antibonding e_g^* and t_{2g}^* levels by a $Q_\theta(\sim 3z^2 - r^2)$ distortion and so $V_E < 0$ for the $^4T_{2g}$ state of CrF_6^{3-} leading to a compressed octahedron as equilibrium geometry. V_E values have been derived from self-consistent charge extended Hückel and MSXα calculations performed at different Q_θ values. The results for the $^4T_{1g}(G)$, $^4T_{2g}(G)$, $^4T_{2g}(D)$, and $^4T_{1g}(P)$ states of MnF_6^{4-} are reasonably close to the experimental figures. For the first excited state $^4T_{1g}(G)$ the value $V_E \approx 60\,cm^{-1}/pm$ found for a metal–ligand distance R equal to 213 pm leads to a Huang-Rhys factor $S_E = 1.5$ also close to experimental findings. On passing from this case to the $^4T_{2g}$ state of CrF_6^{3-} $|V_E|$ increases by a factor of about two but $S_E = 1.2$ in agreement with experimental data for Rb_2KGaF_6: Cr^{3+}. The latter figure implies a Stokes shift $E_S^0(E)$ due to the E_g mode equal to $1200\,cm^{-1}$ which is about 50% of the total Stokes shift. As a salient feature it is shown that for both MnF_6^{4-} and CrF_6^{3-} complexes V_E strongly depends upon R, as it also happens to the V_A coupling constant with the symmetric A_{1g} mode. This reasonably explains the increase of the Stokes shift upon increasing R recently observed for Mn^{2+}-doped fluoroperovskites. Although pure crystal-field (CF) theory gives rise to V_E values much smaller than the experimental ones it is shown that the relation $V_A/V_E = \sqrt{2}$ derived for the first excited state of MnF_6^{4-} and CrF_6^{3-} is not far from the results obtained through MO calculations.

1. Introduction

Photoluminescence is one of the most attractive phenomena associated with transition metal (TM) impurities in insulators. In this process an optical absorption band peaked at energy E_a gives rise to an emission band whose maximum is not at E_a but at $E_e < E_a$. Since the first explanation of this experimental fact (known as Stokes rule) through the concepts of photon and energy conservation [1] models have been proposed to explain the microscopic origin of the difference $E_a - E_e$ (usually called Stokes shift) in terms of a local lattice relaxation [2 to 6]. Because of this the equilibrium metal–ligand distance changes when we go from an electronic state to another one n, as the associate

[1]) Avda. de los Castros, E-39005 Santander, Spain.

energy $E_n(\{Q_k\})$ is in fact a function of the normal coordinates $\{Q_k\}$ of the involved nuclei. Such coordinates are assumed to be the same for any electronic state. The values $\{Q_k\} \equiv 0$ correspond to the equilibrium situation for the electronic ground state.

If we consider in principle an orbitally singlet excited state, its energy $E_n(\{Q_k\})$ can be written as

$$E_n(\{Q_k\}) = E_{n^+}^0 + \sum_k \{V_{nk}Q_k + \tfrac{1}{2}\,\mu\omega_{nk}^2 Q_k^2 + \ldots\}\,, \tag{1}$$

while for the ground state $E_0(\{Q_k\})$ has the form

$$E_0(\{Q_k\}) = E_0^0 + \sum_k \{\tfrac{1}{2}\,\mu\omega_{0k}^2 Q_k^2 + \ldots\}\,. \tag{2}$$

The dependence on $\{Q_k\}$ of the energies comes from the corresponding dependence of the adiabatic Hamiltonian $H(\mathbf{r}, \{Q_k\})$, which can simply be written as

$$H(\mathbf{r}, \{Q_k\}) = H(\mathbf{r}, 0) + \sum_k (\partial V/\partial Q_k)\, Q_k + \ldots\,. \tag{3}$$

If only the linear term in $\{Q_k\}$ is retained in (3) we are working in the so-called *linear* electron–phonon coupling regime. In this regime $\omega_{nk} = \omega_{0k} \equiv \omega_k$ and the minimum value of $E_n(\{Q_k\})$ appears at the coordinates $\{Q_{nk}^0\}$ given by

$$Q_{nk}^0 = -\frac{V_{nk}}{\mu\omega_k^2}\,. \tag{4}$$

Thus, $E_n(\{Q_{nk}^0\})$ is equal to

$$E_n(\{Q_{nk}^0\}) = E_n^0 - \sum_k S_{nk}\hbar\omega_k\,,$$

$$S_{nk}\hbar\omega_k = \frac{V_{nk}^2}{2\mu\omega_k^2}\,, \tag{5}$$

where S_{nk} depicts the Huang-Rhys factors associated with the n-th electronic excited state and the k-th vibrational mode. Within this scheme, if the maximum of an absorption band appears at $E_n^0 - E_0^0$ (following the Franck-Condon principle), the corresponding emission peak corresponds to $E_n(\{Q_{nk}^0\}) - E_0(\{Q_{nk}^0\})$ and thus the Stokes shift is just given [5] by

$$E_S^0 = 2\sum_k S_{nk}\hbar\omega_k\,. \tag{6}$$

If the electronic transition is not allowed but *assisted* [7, 8] by an odd phonon of frequency $\omega_u/2\pi$, then the final expression for the Stokes shift becomes

$$E_S = E_S^0 + \Delta E_u\,,$$

$$\Delta E_u = 2\hbar\omega_u \tanh\,(\hbar\omega_u/2kT)\,. \tag{7}$$

Therefore, to gain a better insight into the experimental Stokes shift a microscopic understanding of the coupling coefficients V_{nk} is required. In the case of TM impurities in insulators it is known that the electronic properties can reasonably be described by means of the MX_p complex formed by the impurity with the p ligands. Moreover, in cases like Cr^{3+}-doped elpasolite lattices the low temperature optical spectra reveal that

coupling occurs with *local* modes of the MX_p complex [9 to 14]. In particular progressions involving the symmetric A_{1g} and the Jahn-Teller E_g modes have been well observed in the $^4T_{2g} \rightarrow {}^4A_{2g}$ electronic transition involving the first excited state $^4T_{2g}$. Moreover, it has been pointed out [7, 10] that the room temperature Stokes shift can essentially be understood *only* through the coupling with the *two stretching* modes A_{1g} and E_g. In other words it can simply be written

$$E_S^0 = E_S^0(A) + E_S^0(E)\,, \tag{8}$$

where

$$E_S^0(A) = 2S_A\hbar\omega_A\,,$$
$$E_S^0(E) = 2S_E\hbar\omega_E\,, \tag{9}$$

and so *only two* coupling constants V_A and V_E related to the first excited state would determine their local relaxation and consequently E_S.

Regarding the coupling coefficient V_A a recent work [8] has investigated its microscopic origin for the first excited states of O_h complexes of Cr^{3+}, Mn^{2+}, and V^{2+} involving halides as ligands. It has been shown [8] that: (i) V_A basically reflects the dependence of the cubic field splitting, $10Dq$, upon the metal–ligand distance R. Such a dependence is usually written as

$$10Dq = CR^{-n} \tag{10}$$

in the vicinity ($\Delta R/R_0 \ll 1$) of R_0, where $R_0 = r(M) + r(X)$ involves the ionic radii of M and X. (ii) The R dependence of $E_S(A)$ in the vicinity of R_0 goes as $R^{6\gamma_A - 2(n+1)}$, where γ_A is the Grüneisen coefficient for the A_{1g} mode. (iii) In the case of O_h complexes of divalent ions like Mn^{2+} or V^{2+}, $E_S(A)$ would increase when R increases.

As regards the latter statement recent experimental results [15] on Mn^{2+}-doped fluoroperovskites unambiguously demonstrate that the total *Stokes shift* E_S at room temperature *increases* as far as the Mn^{2+}–F^- *distance increases.*

Having in mind all these facts a main goal of the present work is not only to calculate V_E as a function of R for the first excited state of CrF_6^{3-} and MnF_6^{4-} complexes but *specially to understand* the microscopic origin of V_E in a direct way. After explaining the calculation procedure in Section 2 it is shown in Section 3 that the calculated values of V_E for several excited states of MnF_6^{4-} and CrF_6^{3-} are close to the experimental values [16, 17]. Moreover, it is possible to explain the observed increase experienced by the Stokes shift of MnF_6^{4-} (and also VCl_6^{4-} [8, 18]) upon increasing R.

2. Theoretical

2.1 Foundations

Linear coupling of electronic states $|T_\mu\rangle$ ($\mu = x, y, z$) (corresponding to an orbital triplet) with a r-degenerate Γ mode (characterized by the normal coordinates Q_α, $\alpha = 1 \ldots r$) requires that not all the matrix elements $\langle T_\mu|\, \partial V/\partial Q_\alpha\, |T_\nu\rangle$ are zero. Thus, as $\partial V/\partial Q_\alpha$ belongs to the Γ representation it must be verified that $T \times T \supset \Gamma$ and so in the case of an octahedral complex A_{1g} and E_g are the only stretching modes which can be linearly coupled to an orbital triplet. The form of $Q_\theta(\sim 3z^2 - r^2)$ and $Q_\varepsilon(\sim x^2 - y^2)$ normal coordinates displaying the Jahn-Teller E_g mode are depicted in Fig. 1.

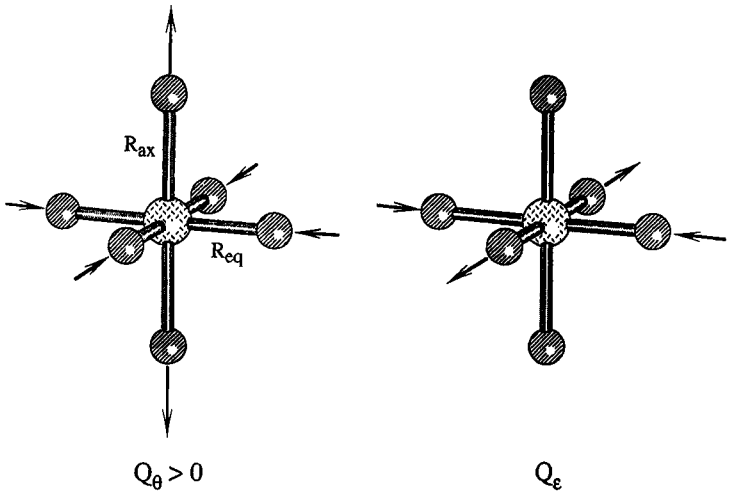

Fig. 1. Picture of the Q_θ and Q_ε normal coordinates corresponding to an octahedral MX_6 complex. R_{ax} and R_{eq} are the axial and equatorial metal–ligand distances, respectively, in D_{4h} symmetry appearing under Q_θ distortion

Under the action of $Q_\theta > 0$ ($Q_\varepsilon = 0$) an octahedron characterized by a metal–ligand distance R gives rise *instantaneously* to an elongated octahedron (D_{4h} symmetry) with two different metal–ligand distances R_{ax} and R_{eq} (defined in Fig. 1) such as $(R_{ax} - R) = -2(R_{eq} - R) = Q_\theta/\sqrt{3}$. To calculate the effects of the linear coupling with the E_g mode within the adiabatic approximation requires to evaluate the twelve matrix elements $\langle T_\mu | \partial V/\partial Q_\alpha | T_\nu \rangle$ ($\alpha = \theta, \varepsilon$). In other words the effects of the electron–phonon coupling term $(\partial V/\partial Q_\alpha)\, Q_\alpha$ (depicted in (3)) *within* the orbital triplet can be described by the Hamiltonian H_{cp} whose expression is given by

$$H_{ep} = \mathbf{V}_\theta Q_\theta + \mathbf{V}_\varepsilon Q_\varepsilon \,, \tag{11}$$

where $\mathbf{V}_\theta$ and $\mathbf{V}_\varepsilon$ are symmetric 3×3 matrices involving $\langle T_\mu | \partial V/\partial Q_\theta | T_\nu \rangle$ and $\langle T_\mu | \partial V/\partial Q_\varepsilon | T_\nu \rangle$ matrix elements, respectively. As H_{ep} must be invariant under O_h group operations applied *simultaneously* on electronic $\mathbf{V}_\theta$ and $\mathbf{V}_\varepsilon$ matrices and normal coordinates Q_θ and Q_ε, this determines all but one of twelve matrix elements. So the mentioned coupling can be described [19] by the simple *effective* Hamiltonian

$$H_{eff} = V_E \{ \mathbf{U}_\theta Q_\theta + \mathbf{U}_\varepsilon Q_\varepsilon \} \,, \tag{12}$$

where

$$\mathbf{U}_\theta = \begin{pmatrix} 1/2 & 0 & 0 \\ 0 & 1/2 & 0 \\ 0 & 0 & -1 \end{pmatrix}, \qquad \mathbf{U}_\varepsilon = \begin{pmatrix} -\sqrt{3}/2 & 0 & 0 \\ 0 & \sqrt{3}/2 & 0 \\ 0 & 0 & 0 \end{pmatrix} \tag{13}$$

operate upon the $|T_x\rangle$, $|T_y\rangle$, and $|T_z\rangle$ wavefunctions. The present problem is thus strongly connected with the changes of the polarizability tensor of an O_h molecule induced by E_g vibrations which appear in the Raman spectroscopy of octahedral complexes.

Adding the elastic energy term $(1/2)\mu\omega_E^2(Q_\theta^2 + Q_\varepsilon^2)$ to (12) the potential energy surfaces display three equivalent minima [19] at

$$\begin{aligned} &\{Q_\theta^0 = q_E,\ Q_\varepsilon^0 = 0\}, \\ &\{Q_\theta^0 = -\tfrac{1}{2}\, q_E,\ Q_\varepsilon^0 = (\sqrt{3}/2)\, q_E\}, \\ &\{Q_\theta^0 = -\tfrac{1}{2}\, q_E,\ Q_\varepsilon^0 = -(\sqrt{3}/2)\, q_E\}; \\ &q_E = V_E/\mu\omega_E^2, \end{aligned} \tag{14}$$

stressing the full cubic symmetry of the problem. The involved decrement of energy is equal to

$$E_{JT} = \tfrac{1}{2}\,\mu\omega_E^2 q_E^2 = \tfrac{1}{2}\,(V_E^2/\mu\omega_E^2) = S_E\hbar\omega_E \tag{15}$$

for each of the three equivalent surfaces.

It is worth noting that the point $\{Q_\theta = 0;\ Q_\varepsilon = 0\}$ is the intersection point of the three surfaces and *not a branch point* [20, 19]. Thus, the E_g mode in the present case behaves as a *potentially* active Jahn-Teller mode according to Toyozawa and Inoue [20]. It means that in the first electronic transition of CrF_6^{3-} or MnF_6^{4-} the resulting band does not exhibit any splitting coming from the Jahn-Teller coupling. Thus, in the present cases the existence of Jahn-Teller coupling in the excited state can be seen *experimentally* through the observation of *progressions* associated with the E_g mode in the low temperature optical spectra [9, 11]. Nevertheless, the *shape* of the optical bands at room temperature is the same as if only the coupling with the *symmetric* A_{1g} modes occurs. This explains the validity of (8) and (9) for the present case in spite of the fact that the excited state is not singlet but degenerate. At the same time (8) and (9) point out that an indirect evidence on the coupling to the E_g mode can also be extracted from the analysis of the experimental Stokes shift as it is discussed in [8].

A further insight into the Jahn-Teller coupling in an orbital triplet thus requires a microscopic interpretation of the coupling constant V_E appearing in the effective Hamiltonian (12). A simple way to do that is exploring the dependence of energies $E_\mu(Q_\theta, Q_\varepsilon)$ on Q_θ associated with the $|T_\mu\rangle$ ($\mu = x, y, z$) states of the triplet. Thus, the comparison between (11) and (12) leads to

$$V_E = -[\partial E_z/\partial Q_\theta]_{Q_\varepsilon = 0} = -[\partial(E_z - E_0)/\partial Q_\theta]_{Q_\varepsilon = 0} = \tfrac{2}{3}\,[\partial(E_x - E_z)/\partial Q_\theta]_{Q_\varepsilon = 0}. \tag{16}$$

So the coupling constant V_E can be determined through the energy variations induced by *static* tetragonal deformations. A deformation is characterized by R_{ax} and R_{eq} (Fig. 1) verifying $(R_{ax} - R) + 2(R_{eq} - R) = 0$.

2.2 Approximations

In the molecular orbital (MO) scheme the electronic state energies of a complex are written in terms of one-electron energies ε_n as well as of matrix elements of the two-electron operator e^2/r_{ij}. In the case of a cubic complex involving a d-cation there are ten independent matrix elements [21]. Usually, however, such matrix elements are written in terms of two effective Racah parameteres B and C. A careful study on MnF_6^{4-} has shown that this approximation is indeed good [22].

Let us now focus upon the dependence of ε_n and Racah parameteres upon the symmetric Q_A coordinate or equivalently upon R. Taking as a guide the case of the MnF_6^{4-} complex in fluoroperovskites it has been shown experimentally [23, 24] and theoretically [22, 25] that: (i) $10Dq$, which is equal to $\varepsilon(e_g^*) - \varepsilon(t_{2g}^*)$ (where e_g^* and t_{2g}^* are the mainly 3d antibonding levels), is strongly sensitive to R changes. (ii) By contrast, the effective Racah parameteres B and C are nearly independent of R.

In view of these results we have assumed that V_E in (12) is essentially determined by the changes undergone by one-electron energies when the Q_θ deformation is switched on. Therefore, if we designate by simplicity as $\{x^2 - y^2, 3z^2 - r^2\}$ and $\{xy, xz, yz\}$ the components of the e_g^* and t_{2g}^* antibonding orbitals, respectively, we need *only* evaluate the changes $\delta\varepsilon(x^2 - y^2)$, $\delta\varepsilon(x, y)$, etc. induced by a Q_θ distortion. Moreover, as a closed shell (displaying A_{1g} symmetry) is not affected by a Q_θ distortion the centre of gravity theorem holds and so

$$\delta\varepsilon\,(x^2 - y^2) + \delta\varepsilon\,(3z^2 - r^2) = 0\,, \qquad \delta\varepsilon(xy) + 2\,\delta\varepsilon\,(xz) = 0\,. \tag{17}$$

2.3 Expression of V_E for the first excited state $^4T_{2g}$ of CrX_6^{3-}

The ground state $^4A_{2g}$ of the CrX_6^{3-} complex arises from the $3d^3$ configuration of isolated Cr^{3+}. Neglecting the mixing with configurations such as $3d^24s$, $3d^24p$, etc. the $M = 3/2$ component of the $|^4A_{2g}\rangle$ wavefunction is just given [21] by the Slater determinant

$$|^4A_{2g}\rangle = |\overset{+}{xy},\ \overset{+}{xz},\ \overset{+}{yz}|\,. \tag{18}$$

The $M = 3/2$ component of the $^4T_{2g}$ state also involves one Slater determinant, and so the $|^4T_{2g},\ z\rangle$ state is described [21] even in a D_{4h} symmetry by the wavefunction

$$|^4T_{2g},\ z\rangle = |\overset{+}{xz},\ \overset{+}{yz},\ x^2 \overset{+}{-} y^2|\,. \tag{19}$$

Thus, by comparison with (18) it involves a jump of an electron placed in the xy π-antibonding orbital to the $x^2 - y^2$ σ-antibonding orbital.

Therefore, applying (16) to the calculation of V_E and assuming that only the changes experienced by one-electron energies are relevant, it is found

$$V_E = [\partial\{\varepsilon(xy) - \varepsilon(x^2 - y^2)\}/\partial Q_\theta]_{Q_\varepsilon = 0} \tag{20}$$

which taking into account (17) becomes

$$V_E = -[\partial\{(1/2)\,\Delta_e - (2/3)\,\Delta_t\}/\partial Q_\theta]_{Q_\varepsilon = 0}\,, \tag{21}$$

where $\Delta_e = \varepsilon(x^2 - y^2) - \varepsilon(3z^2 - r^2)$ and $\Delta_t = \varepsilon(xy) - \varepsilon(xz;\ yz)$ are the splittings induced upon e_g^* and t_{2g}^* orbitals by the Q_θ deformation along $(Q_\varepsilon = 0)$.

Therefore, as the splitting is much bigger for the e_g^* levels (involving σ bonding) than for the t_{2g}^* levels (where π bonding is present) and Δ_e is positive when $R_{ax} > R_{eq}$ (and thus $Q_\theta > 0$), it is expected to compute a negative value for V_E corresponding to the $^4T_{2g}$ excited state of CrX_6^{3-} complexes. In other words taking into account (14) the equilibrium geometry at the three equivalent minima would correspond to a compressed octahedron.

2.4 Expression of V_E for the first excited state $^4T_{1g}(G)$ of MnF_6^{4-}

The situation for this state is a little more complex than for the $^4T_{2g}$ state of CrX_6^{3-} as it involves a mixing of three different configurations: $t_{2g}^4e_g$, $t_{2g}^3e_g^2$, and $t_{2g}^2e_g^3$. Fortunately the amount of $t_{2g}^4e_g^1$ configuration is 95% [17] and so we can discard the configuration interaction in a first approximation. If the $M = 5/2$ component of the $|^6A_{1g}\rangle$ ground state wavefunction is described by the Slater determinant

$$|^6A_{1g}\rangle = |\overset{+}{xy}, \overset{+}{xz}, \overset{+}{yz}, 3z^2 \overset{+}{-} r^2, x^2 \overset{+}{-} y^2| , \tag{22}$$

then the $M = 3/2$ component of the $|^4T_{1g}(G), z\rangle$ wavefunction is given [17] even in D_{4h} geometry by

$$|^4T_{1g}(G), z\rangle = |t_{2g}^4e_g; {}^4T_{1g}, z\rangle = |\overset{+}{xy}, \overset{-}{xy}, \overset{+}{xz}, \overset{+}{yz}, 3z^2 \overset{+}{-} r^2| . \tag{23}$$

Thus, comparing (22) and (23) we see that there is a $x^2 - y^2 \rightarrow xy$ jump on passing from the ground to the excited state. This is the opposite situation to that found in Section 2.3 and thus the expression for V_E is just given by

$$\begin{aligned} V_E(^4T_{1g}(G)) &= -[\partial\{\varepsilon(xy) - \varepsilon(x^2 - y^2)\}/\partial Q_\theta]_{Q_\varepsilon = 0} \\ &= [\partial\{(1/2)\Delta_e - (2/3)\Delta_t\}/\partial Q_\theta]_{Q_\varepsilon = 0} . \end{aligned} \tag{24}$$

Therefore V_E would be positive for this case as it has been measured by Solomon and McClure [17].

2.5 The crystal-field approach

Electronic levels of a MX_6 complex, like t_{2g}^* and e_g^*, are molecular orbitals and so for instance the wavefunction corresponding to t_{2g}^* can be briefly written as

$$|t_{2g}^*\rangle = N\{|d\rangle - \lambda_\pi |\chi_\pi\rangle\} , \tag{25}$$

where $|d\rangle$ belongs to the central ion and $|\chi_\pi\rangle$ is a suitable LCAO of valence π ligand orbitals.

Despite this fact it is also true that the crystal field approach is usually taken as a *reference* model [21]. Thus, we report here the values of V_E obtained in the crystal-field approach for the cases discussed in Sections 2.3 and 2.4. The expressions reported in [17] contain some mistakes with respect to the present ones.

If an octahedral complex whose metal–ligand distance is R is slightly distorted by Q_θ deformation leading to $(R_{ax} - R) = -2(R_{eq} - R) = Q_\theta/\sqrt{3}$ then the shift energy experienced by $x^2 - y^2$ and xy levels is just given by

$$\begin{aligned} \delta\varepsilon(x^2 - y^2) &= Z_L e^2[\{(25/7)\langle r^4\rangle_d/R^6\} - \{(36/7)\langle r^2\rangle_d/R^4\}](R_{eq} - R) , \\ \delta\varepsilon(xy) &= Z_L e^2[\{(100/21)\langle r^4\rangle_d/R^6\} - \{(36/7)\langle r^2\rangle_d/R^4\}](R_{eq} - R) , \end{aligned} \tag{26}$$

where $Z_L e$ is the ligand charge. Shift energies like $\delta\varepsilon(3z^2 - r^2)$ or $\delta\varepsilon(xz)$ are obtained from (17) and (26).

Therefore, for the $^4T_{2g}$ state of CrF_6^{3-} V_E becomes equal to

$$V_E = -(25\sqrt{3}/18)\, Z_L e^2 \langle r^4\rangle_d / R^6 \tag{27}$$

and thus it is negative indeed. It is worth noting that V_E is independent of $\langle r^2\rangle_d$ and then connected to the coupling coefficient V_A for the symmetric A_{1g} mode. Calling $E_{n0} = E_n^0 - E_0^0$, V_A for the present case is just given [8] by

$$V_A = \partial E_{n0}/\partial Q_A = (1/\sqrt{6})\,(\partial 10Dq/\partial R) \tag{28}$$

and so for the $^4T_{2g}$ state of CrX_6^{3-} in the crystal field model V_A becomes

$$V_A = -(25/3\sqrt{6})\,Z_L e^2\langle r^4\rangle_d/R^6 = -(5/\sqrt{6})\,(10Dq/R)\,, \tag{29}$$

where

$$10Dq = (5/3)\,Z_L e^2\langle r^4\rangle_d/R^5\,. \tag{30}$$

Therefore, comparing (27) and (29) the following relation is found:

$$V_A = \sqrt{2}\,V_E\,. \tag{31}$$

In the case of MnX_6^{4-} complexes, as the first excited state $^4T_{1g}$ is essentially described by a $t_{2g}^4e_g$ configuration, it involves a $e_g \rightarrow t_{2g}$ jump and so V_A is given by

$$V_A = -(1/\sqrt{6})\,(\partial 10Dq/\partial R) \tag{32}$$

and thus relation (31) also holds. Applying (31) and (32) to MnF_6^{4-}, putting $\langle r^4\rangle_d = 5.286$ a.u. [26] and $R = 213$ pm $V_E = 12\ \mathrm{cm^{-1}/pm}$ and $10Dq = 1826\ \mathrm{cm^{-1}}$ is found. The comparison with experimental values for $RbMnF_3$ [17, 24], $V_E = 65\ \mathrm{cm^{-1}/pm}$ and $10Dq = 7500\ \mathrm{cm^{-1}}$, underlines the inadequacy of the crystal-field theory for quantitative purposes. In fact a quantity like $10Dq$ mainly reflects the *different chemical bonding* displayed by t_{2g}^* and e_g^* orbitals, which is not taken into account in the crystal-field framework.

2.6 Higher excited states of MnF_6^{4-}: $^4T_{2g}(G)$, $^4T_{2g}(D)$, and $^4T_{1g}(P)$

Let us start discussing the second excited state $^4T_{2g}(G)$. The wavefunction for this state is certainly more complex than that for $^4T_{1g}(G)$ as it involves an important mixing of $t_{2g}^4e_g$, $t_{2g}^3e_g^2$, and $t_{2g}^2e_g^3$ configurations though the first one is the dominant. Therefore, the $|^4T_{2g}(G),\ z\rangle$ wavefunction for this case can be briefly written [17] as

$$|^4T_{2g}(G),\ z\rangle = a\,|t_{2g}^4e_g;\ ^4T_{2g},\ z\rangle + b\,|t_{2g}^3e_g^2;\ ^4T_{2g},\ z\rangle + c\,|t_{2g}^2e_g^3;\ ^4T_{2g},\ z\rangle\,, \tag{33}$$

where the $M = 3/2$ components are given by

$$|t_{2g}^4e_g;\ ^4T_{2g},\ z\rangle = \left|\overset{+}{yz},\ \overset{+}{xz},\ \overset{+}{xy},\ \overset{-}{xy},\ x^2 \overset{+}{-} y^2\right|, \tag{34}$$

$$|t_{2g}^2e_g^3;\ ^4T_{2g},\ z\rangle = \left|\overset{+}{xz},\ \overset{+}{yz},\ 3z^2 \overset{+}{-} r^2,\ 3z^2 \overset{-}{-} r^2,\ x^2 \overset{+}{-} y^2\right|, \tag{35}$$

and the contribution of $|t_{2g}^3e_g^2;\ ^4T_{2g},\ z\rangle$ to (33) is unimportant. So by comparison with the ground state, (34) involves a $3z^2 - r^2 \rightarrow xy$ jump, while (35) involves the opposite $xy \rightarrow 3z^2 - r^2$ jump. Therefore, for the $^4T_{2g}(G)$ state of MnF_6^{4-} the Jahn-Teller coupling coefficient V_E can be written as follows:

$$V_E(^4T_{2g}(G)) = (a^2 - c^2)\,[\partial\{\varepsilon(3z^2 - r^2) - \varepsilon(xy)\}/\partial Q_\theta]_{Q_\varepsilon = 0} \tag{36}$$

or, in terms of Δ_e and Δ_t,

$$V_E(^4T_{2g}(G)) = -(a^2 - c^2)\,[\partial\{(1/2)\,\Delta_e + (2/3)\Delta_t\}/\partial Q_\theta]_{Q_\varepsilon = 0}\,. \tag{37}$$

This expression points out that the admixture of the $t_{2g}^2e_g^3$ configuration (and also $t_{2g}^3e_g^2$) in the $t_{2g}^4e_g$ one tends to decrease the V_E value expected for the case where $|^4T_{2g}(G), z\rangle$ is just described by $|t_{2g}^4e_g; {}^4T_{2g}, z\rangle$ alone ($a = 1$). Moreover, as $t_{2g}^4e_g$ is the dominant contribution in the $^4T_{2g}(G)$ state, equation (37) implies that V_E is negative in qualitative agreement with the measurements reported by Solomon and McClure [17].

As regards now the $^4T_{2g}(D)$ state it is important to remark that the wavefunction $|^4T_{2g}(D), z\rangle$ is also described by (33) though with *different mixing coefficients* a, b, and c from those found for $^4T_{2g}(G)$. Therefore equation (37) can also be applied to calculate V_E for $^4T_{2g}(D)$.

Different from what is found for the first excited state $^4T_{1g}(G)$, in $^4T_{1g}(P)$ there is a significant configuration mixing where $t_{2g}^2e_g^3$ is the dominant one [17]. As

$$|t_{2g}^2e_g^3; {}^4T_{1g}, z\rangle = |\overset{+}{yz}, \overset{+}{xz}, 3z^2 \overset{+}{-} r^2, x^2 \overset{+}{-} y^2, x^2 \overset{-}{-} y^2| \tag{38}$$

it involves (when compared to the wavefunction (22) of the ground state) a $xy \rightarrow x^2 - y^2$ jump. Thus, if $|^4T_{1g}(G), z\rangle$ is written as

$$|^4T_{1g}(G), z\rangle = a\,|t_{2g}^4e_g; {}^4T_{1g}, z\rangle + b\,|t_{2g}^3e_g^2; {}^4T_{1g}, z\rangle + c\,|t_{2g}^2e_g^3; {}^4T_{1g}, z\rangle\,, \tag{39}$$

following a similar procedure to that developed for $^4T_{2g}$ states, it is finally found

$$V_E(^4T_{1g}(P)) = (a^2 - c^2)\,[\partial\{(1/2)\,\Delta_e - (2/3)\,\Delta_t\}/\partial Q_\theta]_{Q_\varepsilon = 0} \tag{40}$$

which coincides with (24) when $a^2 = 1$. As for $^4T_{1g}(P)$ $c^2 > a^2$ [17], V_E would be negative in qualitative agreement with experimental measurements [17].

3. Results and Discussion

3.1 Calculation methods

Calculation of one-electron energies has been carried out for isolated MnF_6^{4-} and CrF_6^{3-} octahedral complexes for three values of the metal–ligand distance $R = 206$, 213, and 220 pm for MnF_6^{4-} and $R = 185$, 191, and 195 pm for CrF_6^{3-}. In order to simulate the Q_θ distortion ($Q_\varepsilon = 0$) of the Jahn-Teller E_g mode coupled to orbital triplet states T we have performed calculations with tetragonal D_{4h} symmetry and so there are two different metal–ligand distances, R_{eq} and R_{ax}. For each value of R four calculations have been made, corresponding to $R_{eq} - R = +2$, $+1$, -1, -2 pm with $R_{ax} - R = -2(R_{eq} - R)$.

To be sure of the predicted trends, two different MO methods have been used simultaneously: the multiple scattered $X\alpha$(MSXα) and the self-consistent charge extended Hückel (SCCEH) methods. The results obtained through *both* methods are *rather similar.*

SCCEH calculations have been carried out following the procedure developed by Ammeter et al. [27] and Bash et al. [28], using accurate Clementi-Roetti [29] wavefunctions. We have verified that the use of poorer-quality wavefunctions significantly affects the dependence of the one-electron splittings Δ_e and Δ_t upon R and Q_θ. In the calculations performed at fixed R but for different Q_θ values only the overlap integrals are varied

and so the relations (17) are reasonably verified. A standard version of the MSXα method [30] has been used for spin-unrestricted calculations. The α parameter for the different atoms was taken from Schwarz's compilation [31]. Sphere radii were chosen according to the Norman procedure [32].

Before accomplishing the present calculations on MnF_6^{4-} and CrF_6^{3-} at different values of the Q_θ coordinate we have verified that *both methods* lead to *reasonable* results concerning the parameters of the *undistorted* octahedral complexes. For instance the $10Dq$ values calculated for MnF_6^{4-} (at $R = 213$ pm) are equal to 7940 cm^{-1} (MSXα) and 7300 cm^{-1} (SCCEH). This value has to be compared with $10Dq = 7260$ cm^{-1} measured for $RbCdF_3$: Mn^{2+} [24], where the Mn^{2+}–F^- distance has been determined to be equal to 213 pm [24, 33]. In the case of CrF_6^{3-} the $10Dq$ values obtained at $R = 191$ pm are equal to 15480 cm^{-1} (SCCEH) and 16250 cm^{-1} (MSXα) and thus not far from $10Dq = 16000$ cm^{-1} for K_2NaGaF_6: Cr^{3+} [13]. We have also verified that the SCCEH and MSXα methods lead to unpaired spin densities not far from experimental ones. A similar situation was found for complexes involving Cu^{2+}, Ag^{2+}, or Ni^+ ions [34, 35] where more details on the employed SCCEH and MSXα methods can be found.

3.2 Results for MnF_6^{4-} at $R = 213$ pm

In Table 1 are collected Δ_e and Δ_t values calculated for different Q_θ values but keeping the same average value of the Mn^{2+}–F^- distance at $R = 213$ pm. It can be seen that both methods give rise to similar results. In particular as expected $|\Delta_e|$ is clearly higher than $|\Delta_t|$.

3.2.1 The first excited state $^4T_{1g}(G)$

Using the data gathered in Table 1 together with (24) the coupling constant V_E can easily be calculated. The results together with the calculated value of the coupling constant V_A for the symmetric A_{1g} mode are reported in Table 2.

It can be noticed that the SCCEH value ($V_E = 63$ cm^{-1}/pm) and the MSXα one ($V_E = 58$ cm^{-1}/pm) for $R = 213$ pm are very close. Moreover, both values lie not far from the experimental one $V_E = 65$ cm^{-1}/pm reported by Solomon and McClure [17] for $RbMnF_3$. Taking now $\hbar\omega = 287$ cm^{-1} [17, 36] and $V_E = 60$ cm^{-1}/pm, equation (15) gives $E_{JT} = 420$ cm^{-1} and $S_E = 1.5$. Such values are consistent with those derived

Table 1

Calculated values of $\Delta_e = \varepsilon(x^2 - y^2) - \varepsilon(3z^2 - r^2)$ and $\Delta_t = \varepsilon(xy) - \varepsilon(xz; yz)$ one-electron splittings for MnF_6^{4-} with D_{4h} geometry keeping the same average value $R = 213$ pm. Results are shown for different values of the $Q_\theta = -2\sqrt{3}\,(R_{eq} - R)$ coordinate, where $R_{ax} + R_{eq} = 3R$. Δ_e and Δ_t are given in cm^{-1} while $R_{eq} - R$ and Q_θ are in pm

		MSXα		SCCEH	
$R_{eq}-R$	Q_θ	Δ_e	Δ_t	Δ_e	Δ_t
2	−6.93	−1190	−310	−1197	−271
1	−3.46	− 588	−146	− 604	−133
−1	3.46	590	143	611	128
−2	6.93	1190	270	1228	252

Table 2
Calculated values of the coupling coefficients V_A and V_E at different metal–ligand distances R corresponding to the first excited state of MnF_6^{4-} ($^4T_{1g}(G)$) and CrF_6^{3-} ($^4T_{2g}$). V_E and V_A are given in cm^{-1}/pm while R is in pm

		MSXα			SCCEH		
system	R	V_A	V_E	V_A/V_E	V_A	V_E	V_A/V_E
MnF_6^{4-}	206	82	71	1.16	108	77	1.40
	213	66	58	1.14	85	63	1.35
	220	58	52	1.12	68	51	1.33
CrF_6^{3-}	185	−170	−141	1.21	−225	−165	1.36
	191	−145	−123	1.18	−182	−130	1.40
	195	−130	−111	1.17	−159	−113	1.41

from the analysis of experimental splitting in the $^4T_{1g}(G)$ state due to spin–orbit coupling, which is significantly reduced by the Ham effect [37]. As the spin–orbit constant λ for the $^4T_{1g}(G)$ state is about 30 cm^{-1} [36], the value $E_{JT} = 420\ cm^{-1}$ explains a posteriori that in this case the Jahn-Teller effect dominates over the spin–orbit interaction.

The values $S_E = 1.5$ and $\hbar\omega_E = 287\ cm^{-1}$ lead to $E_S^0(E) = 860\ cm^{-1}$. This value can be compared with the room temperature experimental value $E_S = 1550\ cm^{-1}$ for $RbCdF_3 : Mn^{2+}$ [15] where the metal–ligand distance R is equal to 213 pm [15]. As the quantity ΔE_u is equal to $\approx 300\ cm^{-1}$ at room temperature for $RbCdF_3 : Mn^{2+}$ [15] the present analysis underlines that $E_S^0(E)$ can be the dominant contribution to the experimental Stokes shift of MnF_6^{4-} in accord with previous conclusions [8].

3.2.2 The excited states $^4T_{2g}(G)$, $^4T_{2g}(D)$, and $^4T_{1g}(P)$ of MnF_6^{4-}

Using the figures given in Table 1 together with expressions (37) and (40) and the values of the coefficients a, b, and c (describing the configuration mixing), the V_E values corresponding to the three states $^4T_{2g}(G)$, $^4T_{2g}(D)$, and $^4T_{1g}(P)$ can be derived. The results are collected in Table 3. The employed coefficients a, b, and c are those given in [17]. Similar values were obtained through the analysis reported in [24]. It can be seen that both the SCCEH and the MSXα methods lead to very similar results as for the

Table 3
Calculated values of V_E for three T excited states of MnF_6^{4-} at $R = 213$ pm compared to the experimental ones reported by Solomon and McClure [17]. The values of the coefficient of configuration mixing $a^2 - c^2$ are also taken from [17]. V_E is given in cm^{-1}/pm

		V_E		
state	$a^2 - c^2$	SCCEH	MSXα	experimental
$^4T_{2g}(G)$	0.53	−59	−59	−36
$^4T_{2g}(D)$	0.25	−28	−28	−23
$^4T_{1g}(P)$	−0.66	−42	−38	−37

$^4T_{1g}(G)$ state.

Despite the approximations involved in the present calculations and the experimental uncertainties the comparison between theoretical and experimental values for the three states can be considered as reasonably good. Moreover, the closeness to experimental values is better in the present case than in the first work reported by Nikiforov et al. [38]. The results collected in Tables 2 and 3, and in Section 3.2.1 support indirectly the validity of the approximations discussed in Section 2.2.

3.3 Results for the $^4T_{2g}$ state of CrF_6^{3-} at R = 191 pm

Table 2 shows that the $|V_E|$ value of CrF_6^{3-} at $R = 191$ is about twice that found for MnF_6^{4-} at $R = 213$ pm. This situation which also holds for V_A can be compared with that experienced by $10Dq$. This quantity also increases by a factor of ≈ 2 on passing from MnF_6^{4-} to CrF_6^{3-} [8].

As no experimental measurements of V_E for CrF_6^{3-} have been reported to our knowledge we can check the validity of the values in Table 2 for CrF_6^{3-} indirectly analysing the obtained values for S_E, E_{JT}, and $E_S^0(E)$. The values collected in Table 4 have been derived using $\hbar\omega_E = 481\ cm^{-1}$ measured [13, 14] for $K_2NaGaF_6 : Cr^{3+}$.

It is worth noting that though V_E for the present case is about twice the value found for the first excited state $^4T_{1g}(G)$ of MnF_6^{4-}, the calculated value of the Huang-Rhys factor is, however, similar for both cases. This comes from the increase usually experienced by the vibrational frequencies on passing from divalent to trivalent complexes [39].

As regards the value of S_E itself it has recently been estimated [40] in $Rb_2KGaF_6 : Cr^{3+}$ through the analysis of the intensities displayed by the peaks corresponding to the E_g vibrational progression. The value given in Table 4 is close to the experimental estimation [40] $S_E = 1.2$. As regards the value of E_{JT} the values collected in Table 4 are not far but a little higher than $E_{JT} = 391\ cm^{-1}$ calculated by Woods et al. [13].

Compared to the room temperature experimental value $E_S = 2800\ cm^{-1}$ reported [13] for $K_2NaGaF_6 : Cr^{3+}$, the value $E_S^0(E) \approx 1200\ cm^{-1}$ derived from Table 4 points out that in the present case the contribution of $E_S^0(E)$ to the total Stokes shift would not exceed 50%. This conclusion is thus in agreement with the analysis carried out in [8] and is supported by the V_A value given in Table 2. In fact taking $V_A = 165\ cm^{-1}/pm$ and using $\hbar\omega_A = 568\ cm^{-1}$ observed experimentally [13, 14] for $K_2NaGaF_6 : Cr^{3+}$ it is found $S_A = 1.3$ and $E_S^0(A) = 1480\ cm^{-1}$.

The present analysis thus supports that the experimental Stokes shift at high temperatures can essentially be understood in terms of coupling only with E_g and A_{1g} modes of the CrF_6^{3-} complex. A similar conclusion emerges from the first calculations on $CrCl_6^{3-}$ using the Amsterdam density functional (ADF) code [41].

Table 4

Values of V_E, S_E, E_{JT}, and $E_S^0(E)$ derived for CrF_6^{3-} at $R = 191$ pm and using $\hbar\omega_E = 481\ cm^{-1}$. E_{JT} and $E_S^0(E)$ are given in cm^{-1} and V_E in cm^{-1}/pm

method	V_E	S_E	E_{JT}	$E_S^0(E)$
SCCEH	−130	1.3	625	1250
MSXα	−120	1.2	575	1150

3.4 V_E for the first excited state of MnF_6^{4-} and CrF_6^{3-}: Dependence on R

The calculated values of V_E (and also of V_A) at different Mn–F and Cr–F distances are also displayed in Table 2. It can be seen that V_E and V_A are both very sensitive to changes of the metal–ligand distance R. Following (10) let us write the dependence of V_E and V_A in the vicinity of R_0 as

$$V_A = C_A R^{-n_A}, \qquad V_E = C_E R^{-n_E}. \tag{41}$$

The calculated exponents n_A and n_E are given in Table 5 for both MnF_6^{4-} and CrF_6^{3-} systems. It is worth noting that

$$n_A = n + 1, \tag{42}$$

where the exponent n was defined in (10).

Aside from telling us that the ratio V_A/V_E is nearly independent of R Tables 2 and 5 reveal that n_A is very close to n_E for both systems and for both employed methods.

Before stressing the importance of this fact concerning the experimental dependence of the Stokes shift upon R for MnF_6^{4-} let us start analysing the variation of the Huang-Rhys factor S_E on going from $KMgF_3 : Mn^{2+}$ to $RbMnF_3$ [36]. In the first case the experimental value is $S_E = 1.35$, while in the second one $S_E = 1.6$ [36]. The equilibrium Mn–F distance for the ground state of $KMgF_3 : Mn^{2+}$ has been determined to be equal to (207 ± 1) pm while $R = 212$ pm for $RbMnF_3$ [23, 24, 33]. Following a previous insight [8] into this kind of problems the increase of S_E upon increasing R can reasonably be explained taking into account (41) and the Grüneisen law for a local mode of the complex written as

$$\frac{\partial(\ln \omega_E)}{\partial(\ln R)} = -3\gamma_E. \tag{43}$$

Therefore taking into account (15), (41), and (43) it is a simple matter to find the R dependence of S_E as follows:

$$S_E \propto R^{9\gamma_E - 2n_E}. \tag{44}$$

Although γ_E has not been determined for complexes involving divalent cations, γ_A has been calculated for MnF_6^{4-} and VF_6^{4-} [25, 42]. The obtained values ($\gamma_A = 2.3$ and 2.9, respectively) indicate that in these cases γ_A lies between 2 and 3. Thus, assuming now that the Grüneisen coefficient γ_E, corresponding also to a stretching mode, lies in the

Tabel 5

Values of the exponents n_A and n_E (defined in (41)) corresponding to the first excited state of MnF_6^{4-} and CrF_6^{3-} complexes calculated by means of SCCEH and MSXα methods

	SCCEH		MSXα	
	n_A	n_E	n_A	n_E
MnF_6^{4-}	7.03	6.26	5.27	4.74
CrF_6^{3-}	6.60	6.52	5.09	4.52

same range as γ_A it becomes possible to understand the increase of S_E when R increases, observed experimentally for MnF_6^{4-} [36]. In fact, taking $n_E = 6.3$ the exponent $9\gamma_E - 2n_E$ which appears in (44) is positive provided $\gamma_E > 1.4$. Assuming for instance $\gamma_E \approx 2.5$, the S_E is proportional to R^{10} and so if $S_E = 1.35$ for $R = 207$ pm, S_E should be close to 1.7 when $R = 212$ pm.

As pointed out in Section 1 recent studies on the room temperature Stokes shift of Mn^{2+}-doped fluoroperovskites have shown [15] that the experimental E_S value also increases significantly as far as R increases following a law $E_S \propto R^{5.3}$.

It was previously pointed out that as

$$E_S^0(A) \propto R^{6\gamma_A - 2n_A} \tag{45}$$

the exponent can be positive if $\gamma_A > 2$, provided we accept $n_A \approx 6$. Nevertheless, in order to well understand the microscopic origin of the observed [15] $E_S \propto R^{5.3}$ dependence for MnF_6^{4-} it is necessary to be sure that $E_S^0(E)$ can exhibit a similar R dependence to that displayed by $E_S^0(A)$. This idea is thus certainly reinforced by the results shown in Table 5 which indicate that n_A and n_E are very close indeed. Although accurate values of γ_A and γ_E are required for further proceeding, the experimental dependence $E_S \propto R^{5.3}$ can be consistent with $\gamma_A = \gamma_E = 2.8$ and $n_A = n_E = 5.7$ as a first approximation. The latter n_A values has been derived from (42) and the value $n = 4.7$ corresponding to the experimental dependence of $10Dq$ upon R in the case of MnF_6^{4-} complexes [23, 24].

It is worth stressing that within the present framework the R dependence of the Stokes shift E_S is strongly sensitive to the actual values of Grüneisen constants γ_A and γ_E. In particular, assuming $\gamma_A = \gamma_E \equiv \gamma$ and $n_A = n_E = 6$, E_S could decrease upon increasing R provided $\gamma < 2$. Though additional experimental data are required first analysis [15] reveals that this is likely the behavior displayed by CrF_6^{3-} complexes in several elpasolite lattices. This is consistent with recent theoretical calculations for CrF_6^{3-} giving values of γ_A lying between 1 and 1.8 [13, 43].

4. Final Remarks

The present work offers a simple way for achieving a better insight into the microscopic origin of signs and absolute values of the coupling constant V_E. The analysis displayed here for several excited states of MnF_6^{4-} and CrF_6^{3-} supports a posteriori that V_E is essentially determined by the energy changes undergone by antibonding one-electron orbitals.

Despite V_E and V_A values calculated within a pure crystal-field approach are substantially smaller than experimental ones it is also true that the relation $V_A/V_E = \sqrt{2}$ derived for the first excited states of MnX_6^{4-} and CrX_6^{3-} complexes is not far from the present MSXα and SCCEH results as is shown in Table 2. This point deserves a further investigation as a possible general relation between V_A and V_E is certainly of interest. In fact V_A can in principle be measured and calculated more easily than V_E.

Aside from obtaining S_E, $E_S^0(E)$, and $E_S^0(A)$ values which are compatible with experimental findings for Mn^{2+} in fluoroperovskites and Cr^{3+} in fluoroelpasolites it is stressed here that the dependence of $E_S^0(E)$ upon R can be very similar to that displayed by $E_S^0(A)$. Thus, this fact provides us with a *reasonable explanation* of the increase experienced by the Stokes shift of Mn^{2+}-doped fluoroperovskites when R increases such as it

has recently been reported in [15]. Having in mind the strong influence of Grüneisen constant γ_A and γ_E on the R dependence of the Stokes shift efforts for a more precise knowledge of them are however required.

The present analysis about the optical properties of Mn^{2+} in fluoroperovskites and Cr^{3+} in fluoroelpasolites is based on theoretical results performed on *isolated* MF_6 units ($M = Mn^{3+}$, Cr^{3+}). This procedure is reasonable provided the electrostatic potential exerted by the rest of the lattice upon the electrons in the complex is perfectly flat. This situation does not always happen as the flatness of such a potential depends on the *type* of crystalline lattice where the complex is embedded. It has been shown [44] that the addition of a non-flat potential on a MF_6 complex modifies the $10Dq$ value and thus it is expected to modify also the constants V_A and V_E. Thus, care has to be taken when comparing V_E, S_E, or $E_S^0(E)$ of a given complex but embedded in two different kinds of host lattices. This point is discussed in [45].

Through the present work it has been pointed out that the R dependence of V_E plays a significant role for understanding that associated with S_E and $E_S^0(E)$. Though the calculated values of n_E appear to give reasonable results it is also necessary to *understand why* V_E is so strongly dependent upon R. This is especially important if we take into account that the pure crystal-field model produces V_E and V_A values much smaller than the experimental ones. Therefore, to try to justify exponents n_E and n_A within a pure crystal-field picture is simply meaningless while the answer to this question has to be sought within the MO description of MnF_6^{4-} and CrF_6^{3-} complexes employed throughout the present paper. First analysis on the R dependence of $10Dq$ within the MO framework reveals [46] that in cases like MnF_6^{4-} or CrF_6^{3-} the *very small amount of 2s orbitals* of F^- in antibonding e_g^* orbitals plays a *crucial role*. Further work along this line is now in progress.

Acknowledgements Fruitful discussions with Dr. F. Rodríguez are acknowledged. This work has been supported by the CICYT under Project No. PB 92-0505.

References

[1] A. Einstein, Ann. Phys. **17**, 132 (1905).
[2] N. F. Mott and R. W. Gurney, Electronic Processes in Ionic Crystals, Chap. 6, Dover Publ. Inc., New York 1940.
[3] K. Huang and A. Rhys, Proc. Roy. Soc. A **204**, 406 (1950).
[4] M. Lax, J. chem. Phys. **20**, 1752 (1952).
[5] J. Bourgoin and M. Lannoo, Point Defects in Semiconductors II, Springer-Verlag, Berlin 1983.
[6] B. Henderson and G. I. Imbusch, Optical Spectroscopy of Inorganic Solids, Chap. 5, 6, Clarendon Press, Oxford 1989.
[7] O. G. Holmes and D. S. McClure, J. chem. Phys. **26**, 1686 (1957).
[8] M. Moreno, M. T. Barriuso, and J. A. Aramburu, J. Phys.: Condensed Matter **4**, 948 (1992).
[9] J. Ferguson, H. J. Guggenheim, and D. L. Wood, J. chem. Phys. **54**, 504 (1971).
[10] H. U. Gudel and T. R. Snellgrove, Inorg. Chem. **17**, 1617 (1978).
[11] R. Knochenmuss, C. Reber, M. U. Rajasekharan, and H. U. Gudel, J. chem. Phys. **85**, 4280 (1986).
[12] M. C. Marco de Lucas, F. Rodríguez, J. M. Dance, M. Moreno, and A. Tressaud, J. Lum. **48/49**, 553 (1991).
[13] A. M. Woods, R. S. Sinkovits, J. C. Charpie, W. L. Huang, R. H. Bartram, and A. R. Rossi, J. Phys. Chem. Solids **54**, 543 (1993).
[14] J. F. Dolan, A. G. Rinzler, L. A. Kappers, and R. H. Bartram, J. Phys. Chem. Solids **53**, 905 (1992).

[15] M. C. Marco de Lucas, F. Rodríguez, and M. Moreno, Phys. Rev. B **50**, 2760 (1994).
[16] M. Y. Chen, D. S. McClure, and E. I. Solomon, Phys. Rev., B **6**, 1690 (1972).
[17] E. I. Solomon and D. S. McClure, Phys. Rev. B **6** 1697 (1972); B **9**, 4690 (1974).
[18] B. Galli, A. Hauser, and H. U. Gudel, Inorg. Chem. **24**, 1697 (1985).
[19] Yu. E. Perlin and B. S. Tsukerblat, The Dynamical Jahn-Teller Effect in Localized Systems, Ed. Yu. E. Perlin and W. Wagner; North-Holland Publ. Co., Amsterdam 1984 and references cited therein.
[20] Y. Toyozawa and M. Inoue, J. Phys. Soc. Japan **21**, 1663 (1966).
[21] S. Sugano, Y. Tanabe, and H. Kamimura, Multiplets of Transition-Metal Ions in Crystals, Academic Press New York 1970.
[22] M. Florez, L. Seijo and L. Pueyo, Phys. Rev. B **34**, 1200 (1986).
[23] F. Rodríguez and M. Moreno, J. chem. Phys. **84**, 692 (1986).
[24] M. C. Marco de Lucas, F. Rodríguez, and M. Moreno, J. Phys.: Condensed Matter **5**, 1437 (1993).
[25] V. Luaña, M. Bermejo, M. Florez, J. M. Recio, and L. Pueyo, J. chem. Phys. **90**, 6409 (1989).
[26] S. Fraga, J. Karwowski, and K. Saxena, Handbook of Atomic Data, Elsevier Publ. Co., Amsterdam 1976.
[27] J. H. Ammeter, A. B. Burgi, J. C. Thibeault, and R. Hoffmann, Amer. Chem. Soc. **100**, 3686 (1978).
[28] H. Bash, A. Viste, and H. B. Gray, J. chem. Phys. **44**, 10 (1966).
[29] E. Clementi and C. Roetti, Atomic Data nuclear Data Tables **14**, 177 (1974).
[30] K. H. Johnson, Adv. Quantum Chem. **7**, 143 (1973).
[31] K. Schwarz, Phys. Rev. B **5**, 2466 (1972).
[32] J. G. Norman, Mol. Phys. **31**, 1191 (1976).
[33] M. T. Barriuso and M. Moreno, Phys. Rev. B **29**, 3623 (1984).
[34] J. A. Aramburu, M. Moreno, and M. T. Barriuso, J. Phys.: Condensed Matter **4**, 9089 (1992).
[35] R. Valiente, J. A. Aramburu, M. T. Barriuso, and M. Moreno, J. Phys.: Condensed Matter **6**, 4515 (1994).
[36] F. Rodríguez, H. Riesen, and H. U. Güdel, J. Lum. **50**, 101 (1991).
[37] F. S. Ham, Phys. Rev. **138**, 1727 (1965).
[38] A. E. Nikiforov, S. Y. U. Shashkin, and A. I. Krotkii, phys. stat. sol. (b) **98**, 289 (1980).
[39] K. Nakamoto, Infrared and Raman Spectra of Inorganic and Coordination Compounds, Wiley, New York 1986.
[40] M. C. Marco de Lucas, Thesis, Universidad de Cantabria 1992.
[41] K. Bellafrouh, C. Daul, H. U. Güdel, F. Gilardoni, and J. Weber, Theor. Chim. Acta **91**, 215 (1995).
[42] N. W. Winter and R. M. Pitzer, J. chem. Phys. **89**, 446 (1988).
[43] L. Seijo, Z. Barandiaran, and L. Pettersson, J. chem. Phys. **98**, 4041 (1993).
[44] K. Pierloot, E. van Praet, and L. G. Vanquickenborne, J. chem. Phys. **96**, 4163 (1992).
[45] M. C. Marco de Lucas, F. Rodríguez, and M. Moreno, phys. stat. sol. (b) **184**, 247 (1994).
[46] M. Moreno, M. T. Barriuso, and J. A. Aramburu, Internat. J. Quantum Chem. **52**, 829 (1994).